Received: 15 February 2024 | Accepted: 8 March 2024

DOI: 10.1002/maco.202414346

ARTICLE

Materials and Corrosion

Evaluating the performance of corn peptone in preventing the corrosion of mild steel immersed in HCl

Taher Rabizadeh

Department of Materials Engineering, Faculty of Mechanical Engineering, University of Tabriz, Tabriz, Iran

Correspondence
Taher Rabizadeh, Department of Materials Engineering, Faculty of Mechanical Engineering, University of Tabriz, Tabriz 51666-16471, Iran.
Email: t.rabizadeh@tabrizu.ac.ir

Funding information
University of Tabriz

Abstract

The effects of biodegradable corn peptone on the corrosion behavior of mild steel in 0.1M HCl were evaluated. The results from the weight loss experiments indicate that changing the amount of corn peptone from 50 to 500 ppm considerably decreased the corrosion rate of the coupons from 28.24 to 4.67 mpy. However, heating the solutions had negative effects on this trend. According to the calculations, dissolving the inhibitor modified the thermodynamic parameters of the corrosion phenomenon. In addition, the adsorption of corn peptone was best fitted with the Langmuir isotherm. The Tafel polarization plots revealed that the presence of corn peptone decreased the corrosion current density from 134.9 to 6.7 $\mu A\ cm^{-2}$. This was compatible with the electrochemical impedance spectroscopy data. Furthermore, X-ray photoelectron spectroscopy analysis confirmed the adsorption of the tested peptone on the surface of the working electrodes, which based on the atomic force microscope images, reduced the surface roughness of the specimens.

KEYWORDS

adsorption, AFM, corrosion, electrochemical impedance spectroscopy, green inhibitor, XPS

1 | INTRODUCTION

Nowadays, mild steel is widely utilized in various industries, especially in petrochemistry, oil, gas, and ore processing, where hydrochloric acid is extensively used to remove any surface impurities (acid pickling process), to dissolve the precipitated mineral scales (oil well acidizing process), and so on.[1] However, exposure to acidic solutions deteriorates the unique properties of mild steel resulting in system shutdowns, contamination of the products, and structural failure.[2] This undesirable phenomenon (also called "corrosion") is a significant concern for both academics and the industry.

Hence, some strategies such as depositing barrier coatings,[3] employing corrosion-resistant materials (i.e., materials selection),[4] and applying cathodic protection[5] have been proposed to minimize the costly consequences of corrosion. However, based on the literature, the addition of particular substances called "corrosion inhibitors" is the most cost-effective and promising one.[6,7]

The efficient industrial corrosion inhibitors are divided into two main groups: inorganics (e.g., chromates, molybdates, and phosphates) and organics (with N and/or S in their molecular structure).[8,9] However, it has been demonstrated that the efficiency of the organic compounds in reducing the corrosion of mild steel in an HCl electrolyte is higher than that of the inorganic ones.[10]

Alkenyl phenones, azoles, acetylenic alcohols, and aromatic aldehydes are the common industrial corrosion

inhibitors used to reduce the destructive effects of corrosion.[11] For instance, the corrosion inhibition efficiency of 5-amino-1,3,4-thiadiazole-2-thiol for mild steel in 1M HCl electrolyte was about 91.5%.[12] One millilitre of dimethylaminocinnamaldehyde as an aldehyde derivative could also reduce the corrosion of mild steel in HCl by 92%.[13]

Here, it should be mentioned that despite the proper performance of the current industrial corrosion inhibitors, most of them are toxic and with numerous environmental side effects.[14] Therefore, the development of biodegradable and eco-friendly corrosion inhibitors has gained attention in recent years.[15] In this regard, plant extracts, pharmaceutical drugs, natural polymers, and proteins are the main candidates.[16] For example, it was observed that 1500 ppm of the powders extracted from the stems of *Eulychnia acida* prevented the deterioration of mild steel in 0.1M HCl by 83%.[17] In another research, an 84% decrease in the corrosion of mild steel in HCl was recorded when 400 ppm norfloxacin as a green drug was added to the system.[18] In terms of the natural polymers and proteins, the corrosion inhibition effects of casein[19] and chitosan[20] in HCl have already been documented. However, no data have been reported on the corrosion inhibition potential of peptones in HCl.

Peptones are protein hydrolysates used in industrial microbial fermentations, for instance, to produce antibiotics.[21] They also contain high amounts of proteins, amino acids, and carbohydrates.[22] Hence, corn peptone, as a sustainable and eco-friendly compound, might be able to decrease the corrosion of mild steel in HCl.

To develop our knowledge, the influence of corn peptone on the corrosion of mild steel in hydrochloric acid was monitored with some electrochemical and surface analysis techniques. It was hypothesized that the molecular structure of corn peptone makes it a potent material in reducing the corrosion rate of the tested metallic coupons.

2 | EXPERIMENTAL PROCEDURE

In this research, the mild steel specimens with the elemental composition (in wt.%) mentioned in Table 1 were employed and subjected to the surface preparation procedure.

TABLE 1 Elemental composition of the tested mild steel pieces (in wt.%).

C	Mn	P	S	Cr	Ni	Fe
0.25	0.95	0.04	0.05	0.3	0.3	Balance

In this regard, the rectangular coupons with the dimensions of about $35 \times 20 \times 2$ mm were (i) abraded with Al_2O_3 abrasive papers from #120 to #2500, (ii) immersed in acetone for 30 s, (iii) rinsed with deionized water for 10 s, and (iv) immediately dried with air.

To prepare the 0.1 HCl electrolyte, an appropriate amount of HCl (37%, Reagent ACS, VWR) was diluted with Mili-Q ultrapure water. The corn peptone-containing solutions were also produced by dissolving 50, 100, 250, or 500 ppm of corn peptone (purchased from Sigma-Aldrich) in the blank solution.

A detailed description of the methods carried out to evaluate the potential of corn peptone in preventing the corrosion of the metallic specimens is provided below.

(i) The weight loss analyses were performed by precisely weighing the as-polished mild steel coupons and then immersing them in the closed vessels containing 250 mL aggressive electrolyte for 24 h. The experiments were conducted using 0.1M HCl without and with different amounts of corn peptone (i.e., 50–500 ppm) at four electrolyte temperatures of 298 K, 313 K, 328 K, and 343 K. The weight of the specimens after 24 h was measured again after removing the corrosion products accumulated on the surface of the coupons and then drying them with the air stream.

(ii) The electrochemical corrosion experiments, including the open-circuit potential (OCP), the electrochemical impedance spectroscopy, and the Tafel polarization method, were carried out at room temperature using a potentiostat/galvanostat (Autolab PGSTAT302N). To perform the corresponding experiments, three electrodes including a counter electrode made of platinum (purity: 99.99%; Ossila Ltd), a saturated calomel electrode (SCE) (Hg/HgCl; Sentek company) as a reference electrode, and a mild steel coupon (with an exposed surface area of 1 cm^2) as a working electrode were placed in a 250 mL high purity borosilicate glass cell (Col¯Int Tech company).

The OCP was recorded immediately after dipping the working electrode in the blank or the corn peptone-containing electrolytes. Each experiment was continued until the corresponding potential versus time plot reached a plateau. The electrochemical impedance spectroscopy analyses were performed at the OCP condition while the frequency changed from 100 000 to 0.01 Hz. During the electrochemical impedance spectroscopy (EIS) measurements, an AC signal of 5 mV was applied. In addition, the required electrochemical EIS data were extracted from the Nyquist and Bode/phase plots using Zview2 software. Finally, the potentiodynamic polarization tests were carried out by changing the potential from −500 to 500 mV versus OCP with a sweep rate of 5 mV s^{-1}. Despite the corrosion potential (E_{corr}) and the corrosion current density (i_{corr}), the anodic (β_a)

and cathodic (β_c) Tafel slopes of the potential versus the logarithm of current graphs were determined using the Tafel extrapolation method.

X-ray photoelectron spectroscopy (XPS; Thermo Escalab 250) was employed to probe the surface layers of the metallic specimens immersed in the corn peptone-free and the 500 ppm corn peptone-containing electrolytes for 24 h at room temperature. The survey spectra were obtained with an aluminum K_α X-ray source. The C (1s) peak detected at 284.8 eV was selected as the reference peak.

The surface characteristics, including the surface topography and the average roughness of the surface polished sample together with those dipping in the blank and the 500 ppm corn peptone-containing corrosive electrolyte for 24 h at room temperature, were determined using an atomic force microscope (AFM; Nanosurf Flex; scanned area: 10×10 μm).

3 | RESULTS AND DISCUSSION

3.1 | Weight loss evaluations

According to the literature, mild steel substances usually experience severe weight loss during the uniform corrosion in HCl.[23] Thus, comparing the changes in the weight of a metallic coupon immersed in the blank and the inhibitor-containing aggressive electrolytes indicates the effectiveness of the dissolved corrosion inhibitor in preventing the corrosion phenomenon.[24] Moreover, the concentration of the inhibitor in the electrolyte and the solution temperature critically affect the degree of inhibition.[25]

In this research, the rate at which the specimens were corroded in the blank (CR_0) and the corn peptone-containing solution (CR) was calculated by considering the changes in the weight of the specimens (i.e., ΔW; in grams) with the surface area of A (cm^2) and density of ρ (in g/cm^3) immersed in the corrosive electrolyte for 24 h (Equation 1).[26]

$$\text{Corrosion rate} = (3.45 \times 10^6 \times \Delta W)/(A \times t \times \rho). \quad (1)$$

The degree of the surface coverage (θ) and the efficiency of corn peptone in inhibiting the corrosion of the specimens (i.e., inhibition efficiency; IE%) were also determined using the below equations.[27]

$$\theta = \frac{CR_0 - CR}{CR_0}, \quad (2)$$

$$IE\% = \theta \times 100. \quad (3)$$

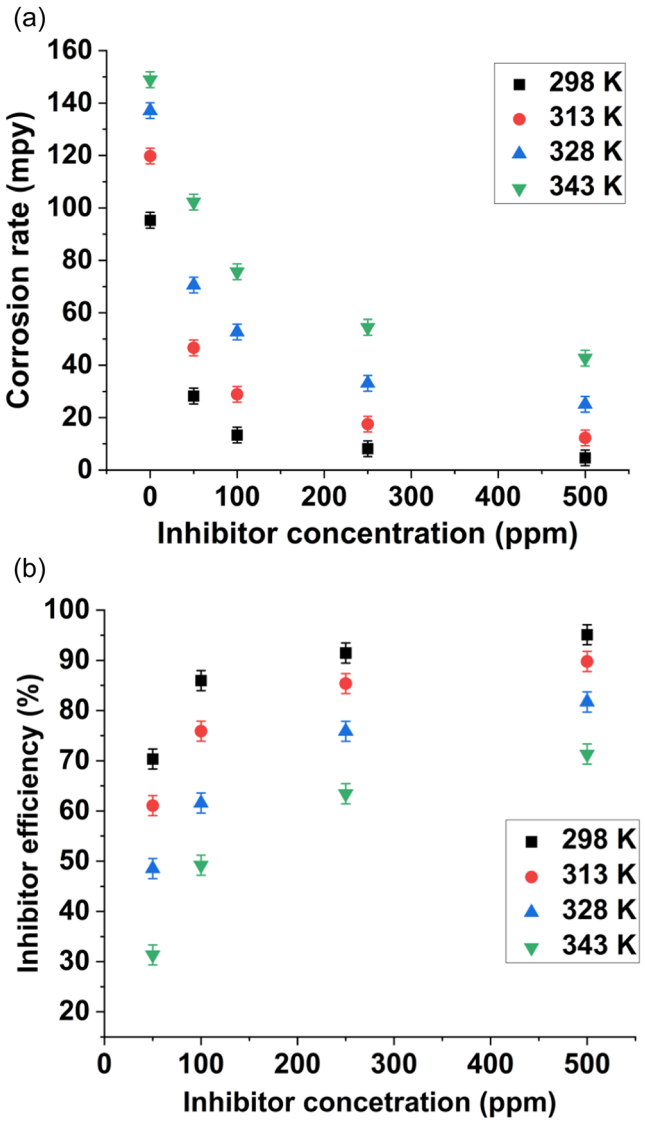

FIGURE 1 (a) CR and (b) IE% values of mild steel coupons after immersion in the blank or the 50–500 ppm corn peptone-amended electrolytes for 24 h at temperatures of 298, 313, 328, and 343 K. [Color figure can be viewed at wileyonlinelibrary.com]

According to the data mentioned in Figure 1 and Table 2, the corrosion rate of the mild steel specimens in the blank corrosive solution at 298 K was 95.30 mpy compared to 28.24 mpy obtained when 50 ppm corn peptone was dissolved in the electrolyte. The observed trend in the corrosion rate continued until the corrosion rate of 4.67 mpy was obtained in the presence of 500 ppm corn peptone. The reason for the measured changes in the corrosion rate is attributed to the adsorption of the tested peptone molecules on the surface of the coupons. Moreover, an increase in the calculated surface coverage (from 0.7 to 0.95) and the corrosion inhibition efficiency (from 70.3% to 95.1%) by increasing the concentration of

TABLE 2 The weight loss data related to the corrosion of mild steel before and after dissolving 50–500 ppm corn peptone at 298–343 K.

Solution temperature (K)	Inhibitor concentration (ppm)	Corrosion rate (mpy)	Surface coverage (θ)	Inhibitor efficiency (%)
298	0	95.30	–	–
	50	28.24	0.70	70.3
	100	13.37	0.85	85.9
	250	8.13	0.91	91.4
	500	4.67	0.95	95.1
313	0	119.8	–	–
	50	46.63	0.61	61.1
	100	28.88	0.75	75.8
	250	17.52	0.85	85.3
	500	12.25	0.89	89.7
328	0	137.1	–	–
	50	70.57	0.48	48.5
	100	52.66	0.61	61.6
	250	33.09	0.75	75.8
	500	25.08	0.81	81.7
343	0	148.9	–	–
	50	102.24	0.31	31.3
	100	75.64	0.49	49.1
	250	54.44	0.63	63.4
	500	42.68	0.71	71.3

corn peptone in the system from 50 to 500 ppm further confirms the suggested mechanism. These findings are in accordance with Yousefi et al., where the geometric blocking phenomena by different types of surfactants and, therefore, a decrease in the corrosion rate of mild steel were illustrated.[28]

Compared to the concentration effect, raising the temperature of the electrolytes from 298 to 343 K had detrimental effects on the corrosion inhibition performance of corn peptone. For example, the corrosion rate of the specimens immersed in the 500 ppm corn peptone-amended electrolyte at 298 K was 4.67 mpy, which dramatically increased to 42.68 mpy when the solution was heated to 343 K (Table 2). There might be some reasons for the negative relationship between the solution temperature and the efficiency of the inhibitor. First, at higher temperatures, the diffusion rate increases while the electrolyte resistance decreases. Second, the inhibitor molecules might decompose, rearrange their configuration, or get desorbed from the surface of the metallic adsorbent.[29]

Assessing the thermodynamic parameters is another method to evaluate the corrosion inhibition characteristics of a chemical compound. Hence, the changes in the corrosion activation energy (E_{act}) together with the entropy (ΔS_{act}) and the enthalpy of activation (ΔH_{act}) related to the corrosion of mild steel specimens immersed in the blank or the corn peptone-containing solutions at temperatures between 298 and 343 K were investigated. With regard to this, the Arrhenius and the transition state theory equations (Equations 4 and 5, respectively) were employed[30]:

$$\mathrm{CR} = A\exp\left(-\frac{E_{act}}{RT}\right), \tag{4}$$

$$\mathrm{CR} = \frac{RT}{\mathrm{Nh}}\exp\left(\frac{\Delta S_{act}}{R}\right)\exp\left(-\frac{\Delta H_{act}}{RT}\right), \tag{5}$$

where A is the frequency factor, R is the universal gas constant, T is the experimental temperature in Kelvin, N is the Avogadro's constant, and h is the Planck's constant.

E_{act} was calculated from the slope of the regression lines added to the [ln CR vs. 1/T] plots (Figure 2a), while the slope and the intercept of the lines best fitted to the [ln(CR/T) vs. 1/T] graphs yielded ΔH_{act} and ΔS_{act},

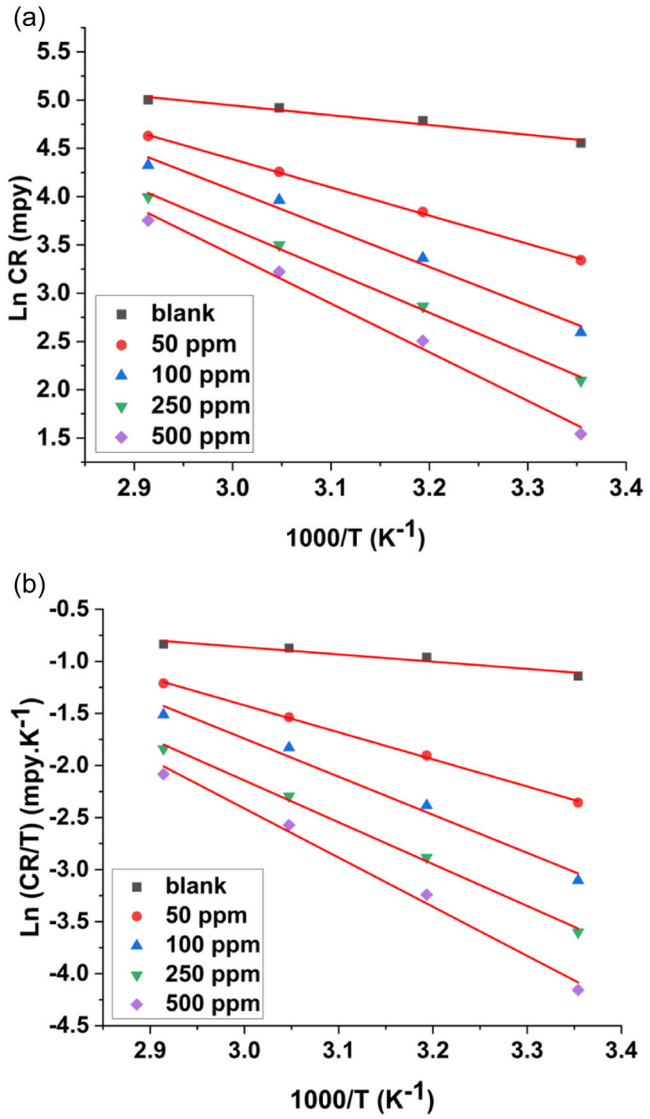

FIGURE 2 (a) Arrhenius and (b) transition state theory plots for the corrosion of mild steel samples dipped in 0.1M HCl containing 0–500 ppm corn peptone at 298, 313, 328, and 343 K. [Color figure can be viewed at wileyonlinelibrary.com]

respectively (Figure 2b). The obtained data are presented in Table 3.

According to this table, dissolving corn peptone in 0.1M HCl increased the E_{act} of the metallic specimens (e.g., from 8.42 kJ mol^{-1} without corn peptone to 41.87 kJ mol^{-1} with 500 ppm of the tested peptone). The observed increase in the energy barrier required for the onset of corrosion was probably due to the adsorption of the additive molecules on the surface of the coupons and, therefore, an increase in the thickness of the double layer established at the metal/solution interface.[31]

Moreover, ΔH_{act} in the presence of corn peptone was much higher than that obtained for the 0.1M HCl solution (5.77 kJ mol^{-1} vs. 39.22 kJ mol^{-1}), which further supports the corrosion inhibition effect of corn peptone.

TABLE 3 The thermodynamic parameters for the corrosion of mild steel samples dipped in 0.1M HCl containing 0–500 ppm corn peptone at 298, 313, 328, and 343 K.

Concentration (ppm)	E_{act} (kJ mol^{-1})	ΔH_{act} (kJ mol^{-1})	ΔS_{act} (J mol^{-1} K^{-1})
Blank	8.42	5.77	−187.4
50	24.27	21.61	−144.5
100	33.05	30.39	−120.8
250	36.04	33.38	−115.2
500	41.87	39.22	−99.9

Furthermore, the negative sign of the entropy of activation reported for the inhibitor-free solution in Table 3 represents an increase in ΔS_{act} during the dissolution of the mild steel specimens. However, the addition of corn peptone decreased the degree of disorder because the peptone molecules substituted for water molecules present on the surface of the specimen.[32] The changes in thermodynamic values were also reported when casein as a natural protein was used to inhibit the corrosion of mild steel in HCl.[19]

3.2 | Adsorption studies

The weight loss data were further analyzed to get better insight into the corrosion inhibition effects of corn peptone and its adsorption on mild steel. Therefore, the concentration of corrosion inhibitor added to the system and the surface coverage values (mentioned in Table 2) were employed to determine the adsorption-desorption equilibrium constant (K_{ads}) of some common adsorption isotherms (Equations 6–9).[33]

$$\frac{C}{\theta} = \frac{1}{k_{ads}} + C\,(\text{Langmuir}), \tag{6}$$

$$\theta = k_{ads} C^{1/n}\,(\text{Freundlich}), \tag{7}$$

$$\exp(f\theta) = k_{ads} C\,(\text{Temkin}), \tag{8}$$

$$\frac{\theta}{[e^{(1-x)} \times (1-\theta)^x]} = k_{ads} C\,(\text{Flory} - \text{Huggins}), \tag{9}$$

where f is the surface energetic inhomogeneity factor and n ($0 < n < 1$) is the heterogeneity parameter.

According to Figure 3, the R^2 values for Langmuir, Freundlich, Temkin, and Flory–Huggins isotherms were 0.999, 0.852, 0.876, and 0.966, respectively, demonstrating that corn peptone adsorption data at 298 K were best fitted to the Langmuir adsorption isotherm.

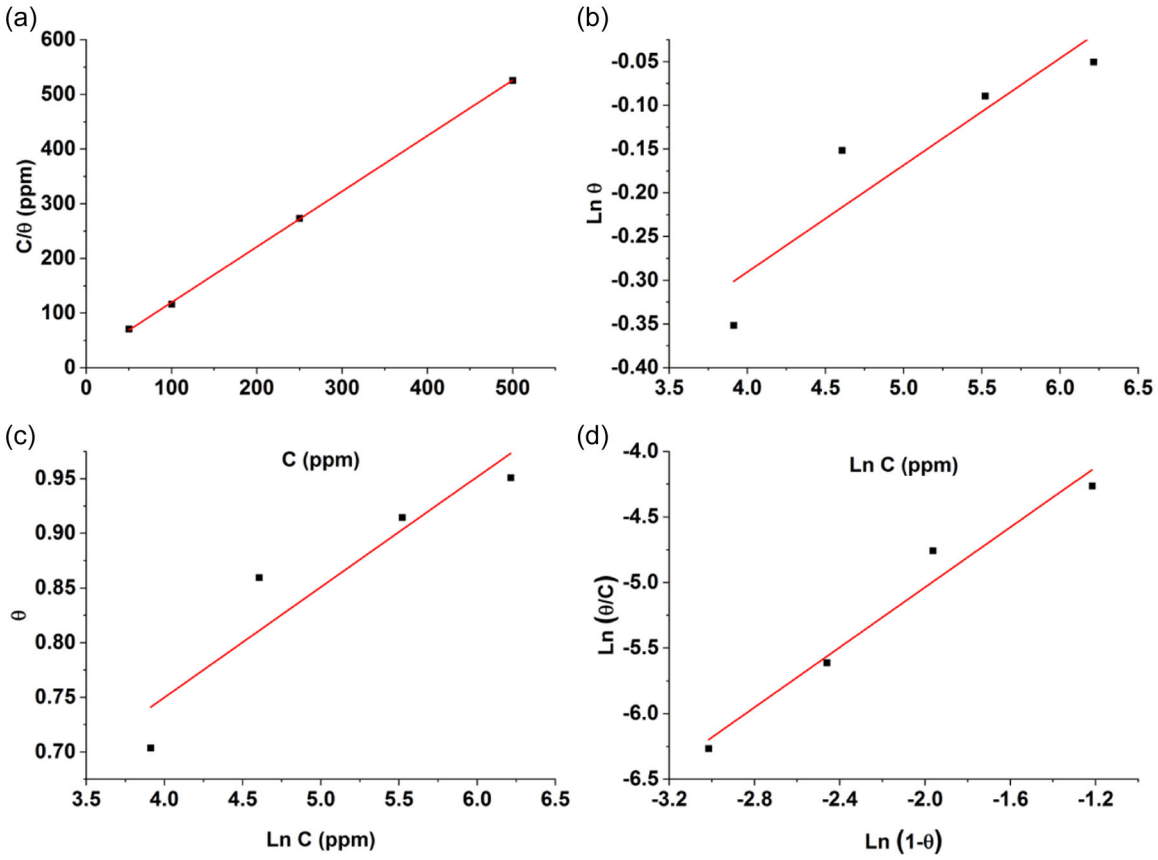

FIGURE 3 Plots for the (a) Langmuir, (b) Freundlich, (c) Temkin, and (d) Flory–Huggins isotherms obtained when mild steel coupons were immersed in the blank or corn peptone-containing solutions at 298 K. [Color figure can be viewed at wileyonlinelibrary.com]

The equation related to the Langmuir adsorption isotherm was also utilized to study the adsorption of corn peptone on the inhibited specimens at higher temperatures (Figure 4). It was noticed that the R^2 values were between 0.99 and 1, indicating that the adsorbed corn peptone molecules formed a monolayer on the surface of the coupons, and they did not interact with each other.[34]

To highlight how increasing temperature might affect the interaction strength between the corn peptone molecules and mild steel, the free energy of adsorption (ΔG°_{ads}) was determined (Equation 7′)[19]:

$$\Delta G^{\circ}_{ads} = -RT \ln(K_{ads} \times C_{solvent}), \qquad (7')$$

where the equilibrium constant of adsorption (K_{ads}) was obtained from the inverse of the intercept of the plots in Figure 4, and $C_{solvent}$ is the molar concentration of the solvent (1000 000 in $mg.l^{-1}$ for water).

Table 4 reveals that increasing the temperature from 298 to 343 K decreased K_{ads} (e.g., from 0.0553 L mg^{-1} at 298 K to 0.011 L mg^{-1}at 343 K) and made ΔG°_{ads} less negative

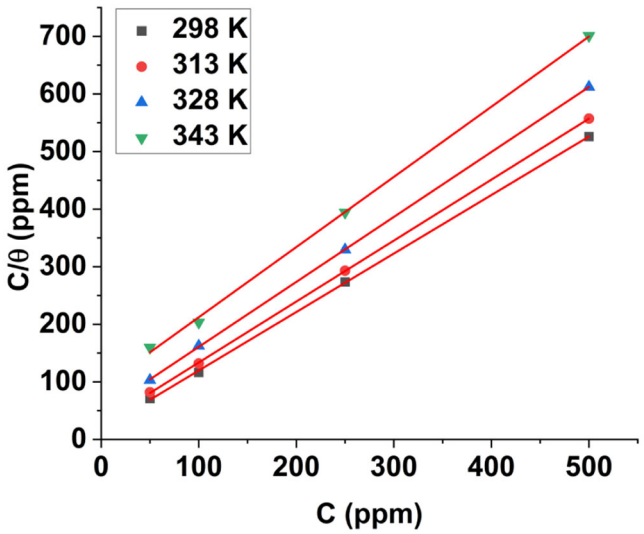

FIGURE 4 Plots for the Langmuir adsorption isotherm when mild steel coupons were immersed in the blank or corn peptone-containing solutions at different temperatures. [Color figure can be viewed at wileyonlinelibrary.com]

TABLE 4 Changes in the corn peptone adsorption data calculated for the inhibition of mild steel in 0.1M HCl at different temperatures.

Temperature (K)	K_{ads} (L mg^{-1})	ΔG°_{ads} (kJ mol^{-1})
298	0.0553	−27.07
313	0.0361	−26.01
328	0.0208	−24.65
343	0.011	−23.1

(e.g., from −27.07 kJ mol^{-1} at 298 K vs. −23.1 kJ mol^{-1} at 343 K). The observed trend indicates that an increase in the solution temperature had undesirable effects on the corrosion inhibition process and desorbed the inhibitor molecules from the surface of the specimens.[20] In addition, the negative sign of ΔG°_{ads} reveals that the inhibitor molecules adsorbed on the coupons spontaneously, and heat was released during this phenomenon.[35]

Furthermore, based on the literature, the ΔG°_{ads} values between zero and −20 kJ mol^{-1} represent the electrostatic interactions between the inhibitor molecules and the metallic substrate (i.e., the physical adsorption). The ΔG°_{ads} values, which are more negative than −40 kJ mol^{-1}, indicate the sharing charges phenomenon (i.e., chemical adsorption). However, both the physical and chemical adsorption take part in the adsorption of the utilized inhibitor if the free energy of adsorption is between −20 and −40 kJ mol^{-1}.[36] As the ΔG°_{ads} values in this research varied between −25.88 and −24.71 kJ mol^{-1} (see Table 4), it can be said that both electrostatic force and charge sharing happened between corn peptone and the metallic pieces.

3.3 | Electrochemical analyses

The ability of corn peptone to reduce the corrosion of mild steel was also investigated by some electrochemical techniques. In this regard, the potential at zero-current (also known as OCP) of the working electrodes immersed in the corrosive electrolyte was recorded in the absence or presence of 50–500 ppm corn peptone (Figure 5). It was observed that the OCP values were not stable during the first 60 min, which was due to the metal dissolution phenomenon that started immediately after immersing the working electrode in the blank electrolyte. However, after about 45 min, the corresponding plot reached the plateau, and the final value of −595 mV was recorded. In comparison, the presence of 50, 100, 250, or 500 ppm corn peptone in the electrolyte shifted the OCP plots toward the positive end-values of −551, −528, −516, and −508 mV, respectively, suggesting the adsorption of the peptone molecules on the tested samples.

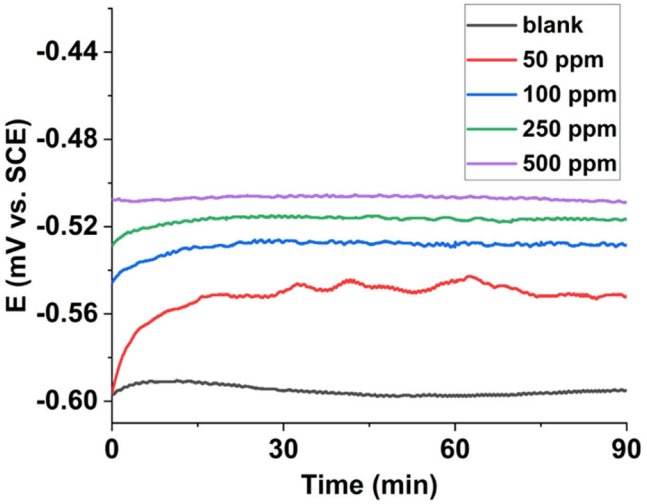

FIGURE 5 The effects of different amounts of corn peptone on the open-circuit potential values of mild steel dipped in 0.1M HCl at room temperature. [Color figure can be viewed at wileyonlinelibrary.com]

Interestingly, in the presence of corn peptone, the OCP developed with different trends than that observed in the 0.1M HCl solution. With 50 ppm corn peptone, the inhibitor molecules gradually adsorbed on the surface of the working electrode; therefore, the OCP value increased from −588 to −551 mV during the first 20 min and stayed almost unchanged after some fluctuations. On the other hand, by increasing the concentration of corn peptone to 100 ppm, it took about 12 min for the OCP plot to start leveling off, and less fluctuation was observed. However, due to the quick adsorption of the protein molecules, the OCP plots obtained with 250 and 500 ppm corn peptone remained almost stable from the time the working electrode dipped into the electrolyte. The formation of a barrier film from the adsorbed inhibitor, which caused an increase in the OCP of a steel substrate has been demonstrated by others.[37]

The corrosion inhibition performance of corn peptone was further evaluated using the potentiodynamic polarization technique, during which an electrical potential was applied on the working electrodes, immersed in the blank or the inhibitor-containing corrosive medium, and the resulting current was measured. According to Figure 6, the potential versus the logarithm of current curves was composed of two active regions, including a cathodic and an anodic branch, where hydrogen/oxygen evolution and the mild steel dissolution reactions took place, respectively.

Moreover, the Tafel extrapolation method was utilized to calculate the corrosion potential (E_{corr}), the corrosion current density (i_{corr}), the Tafel slopes, and the polarization resistance of the working electrodes in the absence and the presence of various milligrams per liter of corn peptone

(Table 5). It can be seen by dissolving corn peptone and increasing its concentration in the electrolyte that the corrosion current density shifted toward lower values (e.g., 139.4 μA cm^{-2} for the blank electrolyte to 6.7 μA cm^{-2} for the 500 ppm peptone-containing system), illustrating that corn peptone reduced the corrosion of the working electrodes in 0.1M HCl.

Based on Table 5, the presence of corn peptone decreased the cathodic and anodic Tafel slopes. According to the surface coverage data mentioned in Table 2, corn peptone adsorbed on the surface of the working electrodes and formed a protective film at the metal/electrolyte interface. Hence, the rate of the hydrogen evolution and the metal dissolution reactions decreased, which highlights the mixed-type nature of the tested inhibitor.[19]

Additionally, prior literature suggests that if the differences in the E_{corr} values measured in the presence and absence of an inhibitor are less than 85 mV, the tested inhibitor is a mixed-type compound. But, if the presence of an inhibitor shifts the E_{corr} values to more than 85 mV, the inhibitor would be identified as either an anodic or cathodic type.[38] In this study, the largest shift in E_{corr} was 83 mV, which was achieved in the presence of 500 ppm corn peptone, indicating the mixed-type feature of the tested peptone. However, as E_{corr} moved toward the positive values (i.e., anodic regions), it can be said that corn peptone was an anodic inhibitor and significantly affected the dissolution reactions of the working electrodes by almost adsorbing on the anodic sites of mild steel.

It is worth noting that the corrosion inhibitors reduce the corrosion rate by increasing the polarization resistance of the working electrodes.[39] Based on Equation (8′), the polarization resistance in the blank solution was 76.5 Ω cm^2, which increased to 1352.6 Ω.cm^2 when 500 ppm peptone was dissolved in the electrolyte.

$$R_P = \frac{(\beta_a \times \beta_c)}{2.303 \times i_{corr} \times (\beta_a + \beta_c)}. \quad (8')$$

The effect of corn peptone on the corrosion of the working electrode in 0.1M HCl was deeply studied using

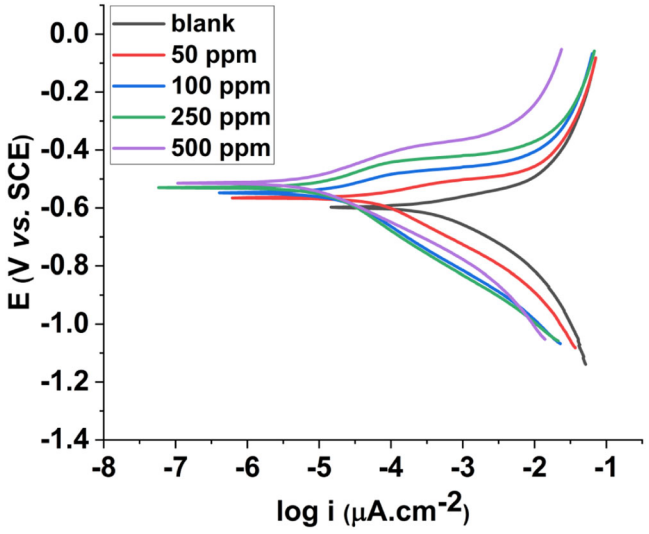

FIGURE 6 The graphs obtained from polarization analyses for the corrosion of mild steel immersed in the blank or the corn peptone-amended solutions at room temperature. [Color figure can be viewed at wileyonlinelibrary.com]

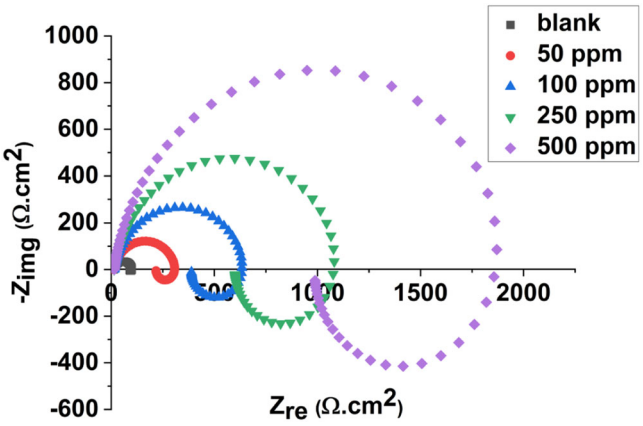

FIGURE 7 Nyquist plots for the corrosion of mild steel dipped in the blank or the corn peptone-amended electrolyte at room temperature. [Color figure can be viewed at wileyonlinelibrary.com]

TABLE 5 The parameters obtained from the polarization curves related to the corrosion of mild steel in the blank or the corn peptone-amended solutions at room temperature.

Concentration (ppm)	E_{corr} (mV vs. SCE)	I_{corr} (μA cm^{-2})	β_a (mV dec^{-1})	$-\beta_c$ (mV dec^{-1})	R_{pol} (Ω cm^2)
Blank	−597.4	134.9	39.4	59.8	76.5
50	−565.5	38.01	37.3	55.7	255.5
100	−547.7	21.2	36.8	53.5	447.1
250	−530.6	12.1	36.3	51.1	762.6
500	−514.5	6.7	35.9	49.7	1352.6

electrochemical impedance spectroscopy. The Nyquist graphs obtained from both corn peptone-free and corn peptone-containing solutions showed one single semicircle and one "pseudo-inductive" loop at high and low frequencies, respectively (Figure 7). However, the diameter of the semicircles increased by dissolving corn peptone in the solution, notifying an increase in the impedance of the corn peptone-inhibited-working electrodes. These results were in line with the data gained from Tafel polarization curves (Figure 6).

It has widely been stated that the appearance of a capacitive loop is because of the resistance to the charge-transferring phenomenon that occurs across the electrode/electrolyte during the corrosion of the working electrode.[40] However, it has been suggested that a pseudo-inductive loop is observed when the corrosion products accumulate on the surface of the working electrode and/or the frequency response is nonlinear. In addition, the relaxation of the charged species like H^+_{ads}, Cl^-_{ads}, and/or inhibitor species adsorbed on the surface of the metallic specimen immersed in the corrosion inhibitor-containing solution can result in such loops in the Nyquist plots.[41] Furthermore, an electrical circuit was designed to analyze the EIS data (Figure 8). The circuit includes different elements, such as R_s and R_{ct}, which represent the solution resistance between the reference electrode and the metallic specimen and the charge transfer resistance at the working electrode/0.1M HCl solution interface, respectively. R_{ct} also determines the diameter of the capacitive semicircle, and an increase in its value indicates a decrease in the corrosion rate of the working electrode.[20]

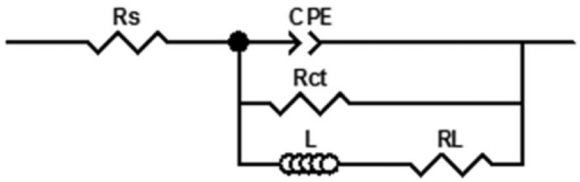

FIGURE 8 The circuit considered to interpret the EIS spectra.

In addition, C_{dl} is usually considered to quantify the capacitance value of the double layer formed at the interface between the working electrode and the corrosive solution. However, an unsmooth and inhomogeneous surface of the working electrode and/or the adsorption of the species present in the solution deviates C_{dl} from the ideal condition.[42] Therefore, in this study, constant phase element (CPE) was employed instead of C_{dl}. CPE is composed of two characteristic parameters, namely CPE-T and n. Considering ω as the angular frequency ($\omega = 2\pi f$; rad.s^{-1}), Y as the magnitude of CPE ($\Omega^{-1}\,S^n\,cm^{-2}$), and $j = (-1)^{1/2}$ as the imaginary number, the impedance of CPE is expressed according to Equation (9′)[43]:

$$Z_{CPE} = Y^{-1}(j\omega)^{-n}. \quad (9')$$

The empirical number n ($0 \le n \le 1$) also signifies the deviation from the ideal capacitive conditions (e.g., C_{dl}).

The inductive resistance ($\Omega\,cm^2$) and the inductance ($H\,cm^2$) elements were also considered in the circuit as R_L and L, respectively. The fitting results, as shown in Table 5, reveal that the R_{ct} values increased from 304.3 to 2018.3 $\Omega\,cm^2$ as the concentration of corn peptone in the corrosive electrolyte increased from 50 to 500 ppm, while the R_{ct} of the corn peptone-free system was determined to be 91.2 $\Omega\,cm^2$.

Furthermore, CPE-T for the sample immersed in the corn peptone-free solution was approximately $3.12 \times 10^{-4}\,\Omega^{-1}\,S^n.cm^{-2}$, about six times higher than the corresponding value obtained for the specimen inhibited

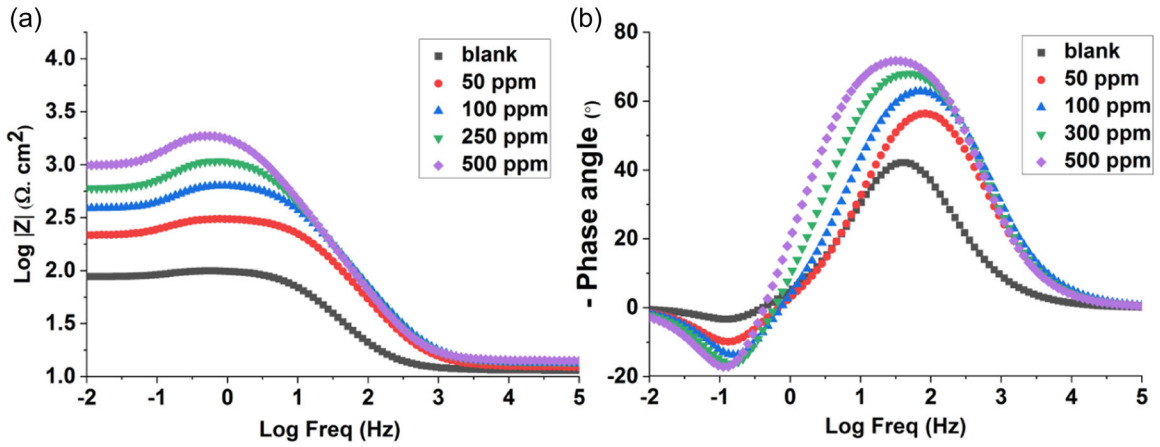

FIGURE 9 (a) Bode and (b) phase angle plots for the corrosion of mild steel in 0.1M HCl in the absence and presence of corn peptone at room temperature. [Color figure can be viewed at wileyonlinelibrary.com]

with 500 ppm corn peptone. The decrease in CPE-T indicates the adsorption of corn peptone molecules on the working electrode, which caused an increase in the thickness of the double layer formed in the vicinity of the immersed specimen.

In addition, the adsorption of the corn peptone molecules made the surface of the metallic substrates more homogeneous and therefore resulted in an increase in the values of n (e.g., from 0.84 for the uninhibited sample to 0.90 for the inhibited with 500 ppm corn peptone).

Furthermore, the presence of the corrosion products on the surface of the uninhibited sample yielded the L and R_L values of 534 H cm^2 and 91.2 Ω cm^2, respectively. However, with 50 ppm corn peptone, $L = 852$ H.cm^2 and $R_L = 304.2$ Ω cm^2 were obtained, while a 10 times increase in the amount of corn peptone dissolved in the electrolyte resulted in a considerable increase in the inductive resistance and the inductance values (e.g., $L = 3038$ H cm^2 and $R_L = 2018.3$ Ω cm^2). Similarly, the other researchers observed an increase in L and R_L when a corrosion inhibitor was added to the corrosive electrolyte.[44]

Besides Nyquist plots, the Bode-phase angle plots displayed the inhibitory action of corn peptone in 0.1M HCl. It has been reported that the magnitude of the impedance (i.e., impedance modulus; $|Z|$) at almost log f = −2 Hz represents the efficiency of a compound in inhibiting the tackling the corrosion.[45] In the case of corn peptone, a shift toward the higher impedance modulus values was noticed when the amount of the inhibitor molecules in the solution increased from 50 to 500 ppm, and the highest log $|Z|$ of 3 was measured with 500 ppm corn peptone (Figure 9a). In addition, the phase-angle plot (Figure 9b) revealed a peak with a maximum at log $f = 1.8$ and one valley at log $f = -0.8$,

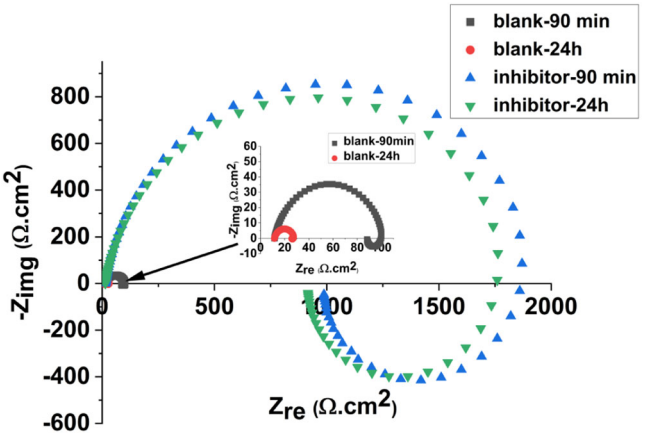

FIGURE 10 Nyquist plots obtained for mild steel dipped in the 0.1M HCl or 500 ppm corn peptone-amended electrolyte for 90 min and 24 h at room temperature. [Color figure can be viewed at wileyonlinelibrary.com]

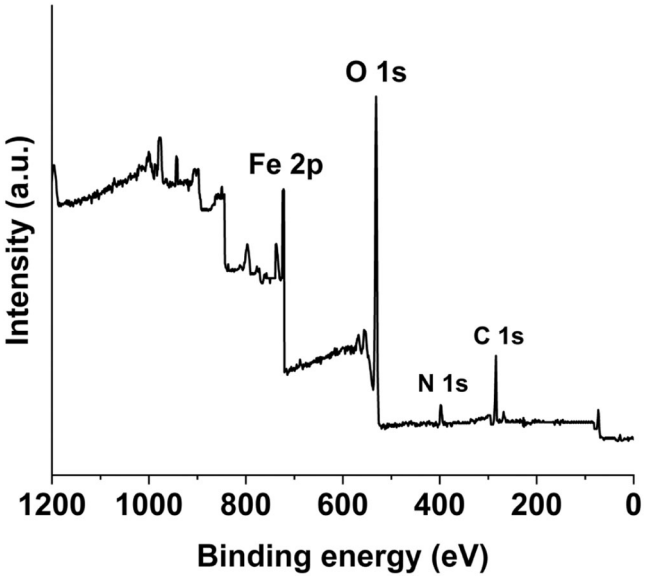

FIGURE 11 X-ray photoelectron spectroscopy (XPS) spectra obtained from the surface of the mild steel specimen exposed to 0.1M HCl containing 500 ppm corn peptone for 24 h at room temperature.

TABLE 6 EIS data for mild steel working electrodes dipped in the blank or corn peptone-amended electrolytes for 90 min and/or 24 h at room temperature.

	R_s (Ω cm^2)	CPE-T (Ω^{-1} S^n cm^{-2})	n	R_{ct} (Ω cm^2)	L (H cm^2)	R_L (Ω cm^2)
Blank–90 min	11.52	3.12×10^{-4}	0.84	91.2	534	477
Blank–24 h	11.5	8.34×10^{-3}	0.81	16.8	254	101
50 ppm–90 min	12.4	7.75×10^{-5}	0.86	304.3	852	623
100 ppm–90 min	13.4	5.35×10^{-5}	0.87	651.4	1062	885
250 ppm–90 min	13.8	5.09×10^{-5}	0.89	1140.1	1572	1201
500 ppm–90 min	14.1	4.88×10^{-5}	0.9	2018.3	3038	1875
500 ppm–24 h	141	4.95×10^{-5}	0.89	1915.4	2534	1702

indicating the occurrence of a capacitive and an inductive loop in the Nyquist graphs, respectively.

The stability of the corn peptone molecules adsorbed on the surface of the metallic specimens, and therefore, their effectiveness in preventing the corrosion of mild steel, was assessed by repeating the EIS measurements for the samples immersed in the inhibitor-free and the 500 ppm corn peptone-amended solutions after 24 h (Figure 10). As indicated in Table 6, immersing the working electrode in the blank solution for 24 h reduced the charge transfer resistance values from 91.2 to 16.8 $\Omega\,cm^2$. In contrast, a slight decrease in the corresponding value (from 2018.3 to 1915.4 $\Omega\,cm^2$) was noticed for the sample exposed to the 500 ppm corn peptone-containing solution emphasizing the potential of corn peptone in tackling the corrosion phenomenon for a long time.

3.4 | XPS evaluations

To elucidate the adsorption of corn peptone, which caused a significant decrease in the corrosion rate of mild steel, the surface of the specimen immersed in the 500 ppm corn peptone amended-electrolyte for 24 h at room temperature was probed by XPS (Figure 11). According to the full survey spectra, the Fe 2p and O 1s signals are present at 74.55 and 531.51 eV, respectively, which originated from the mild steel coupon. In addition, one N 1s peak at 399.37 eV was detected, which was due to the adsorption of corn peptone-containing amine functional groups on the surface of the metallic coupon. The other researchers could also demonstrate the adsorption of a nitrogen-containing corrosion inhibitor on the surface of carbon steel specimens by observing an N 1s peak in the XPS spectra.[46]

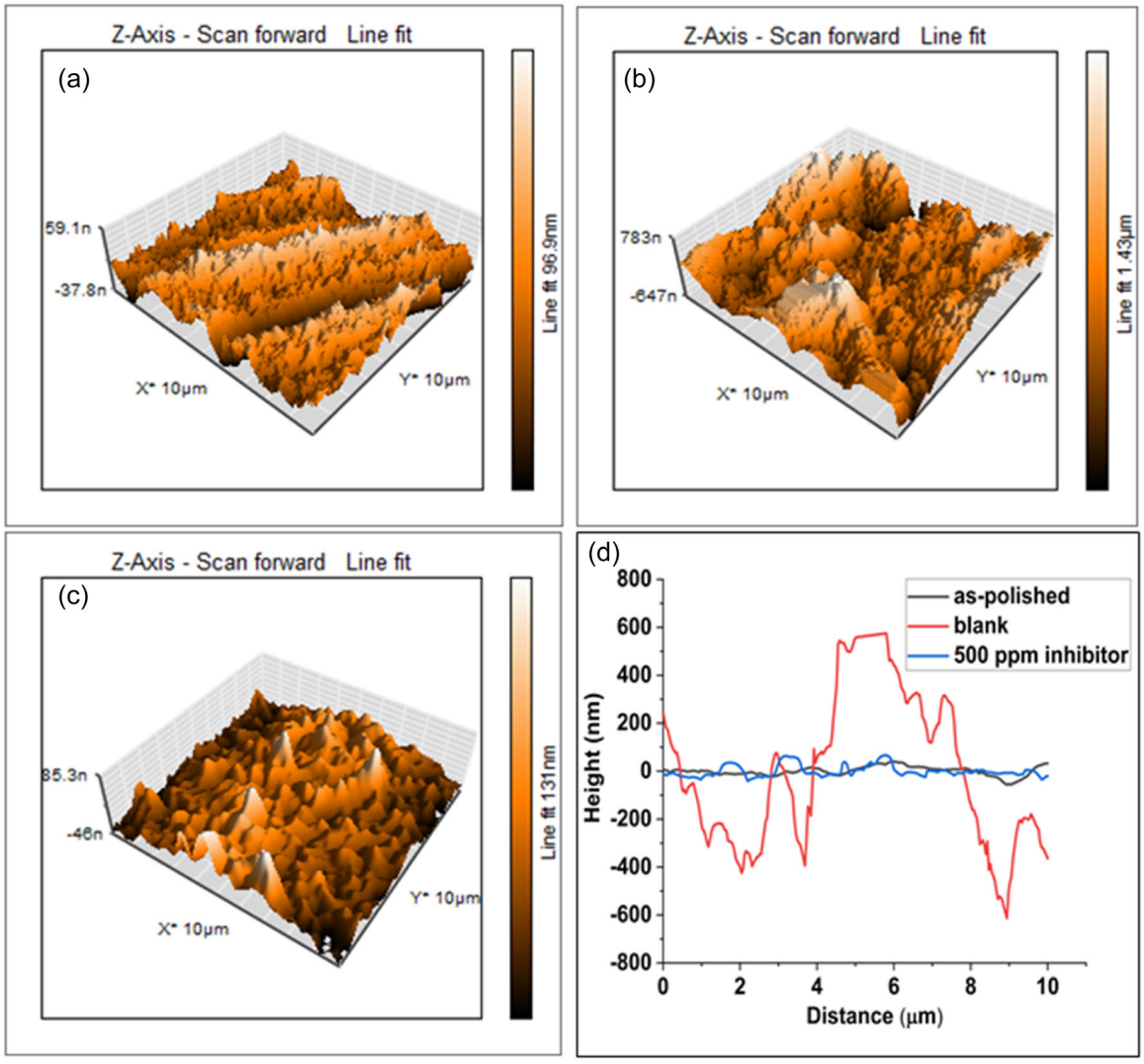

FIGURE 12 Surface topography evaluations of the mild steel coupons: (a) the as-grinded, (b) dipped in blank solution at room temperature for 24 h, and (c) dipped in the 500 ppm corn peptone-amended solution at room temperature for 24 h; (d) the corresponding height profiles for the coupons. [Color figure can be viewed at wileyonlinelibrary.com]

The surface topography and the surface roughness of the mirror surface finished mild steel specimen, and those immersed in the blank or 500 ppm corn peptone-containing solutions for 24 h at room temperature were evaluated using AFM. According to Figure 12, just minor scratches were detected on the surface of the as-grinded coupon (Figure 12a). However, the sample immersed in the peptone-free solution was extremely uneven, while the dissolving 500 ppm corn peptone in the electrolyte yielded an approximately flat surface with very little degradation (Figure 12b vs. 12c). The observed differences in the surface quality of the specimens were further confirmed by measuring the corresponding Ra value (Figure 11d). As can be seen in the height profile, the line graph of the as-polished sample was almost flat (Ra = about 40), similar to the graph obtained for the sample inhibited by 500 ppm corn peptone. However, very sharp peaks (Ra = about 600) were recorded for the uninhibited coupon stating the occurrence of intensive corrosion due to the lack of any surface protective film in the absence of corn peptone. A decrease in the surface roughness of the carbon steel coupons in the presence of a corrosion inhibitor has been noticed elsewhere.[47]

3.5 | Mechanism of inhibition

As stated above, corn peptone could reduce the corrosion rate of mild steel immersed in 0.1M HCl electrolyte via both physisorption and chemisorption phenomena. The primary factors that influenced the corrosion inhibition of the coupons by corn peptone were the surface charge of metal in the hydrochloric acid solution and the molecular structure of corn peptone.

It has been reported that a positive surface charge is created on the surface of the specimens immersed in an acidic environment, which causes the surface adsorption of Cl^- present in the solution. This results in the accumulation of a negative charge on the surface of the working electrodes, which facilitates the adsorption of the protonated functional groups (e.g., NH_2^+) of the corrosion inhibitor (in this research: corn peptone) through an electrostatic attraction (also called physisorption).[48] In terms of chemisorption, oxygen heteroatoms donate their unshared valence electrons to the empty 3d-orbitals of Fe atoms of the mild steel.[49]

4 | CONCLUSION

This study explored the potential of corn peptone as an effective biodegradable compound for inhibiting the corrosion of mild steel in 0.1M HCl solution. The results showed that increasing the amount of corn peptone from 50 to 500 ppm in the corrosive electrolyte led to a significant decrease in the weight loss and the corrosion rate of the steel coupons. This was related to the surface adsorption of corn peptone, which was confirmed by XPS analysis. However, the inhibitory performance of the tested peptone decreased when the temperature of the solution increased from 298 to 343 K. Thermodynamic findings indicated that corn peptone adsorbed on the specimen surface through both physical (electrostatic interaction) and chemical (charge sharing) adsorption processes, resulting in an increase in the activation energy for corrosion and enthalpy of activation. The Langmuir adsorption isotherm was found to govern the selective adsorption of the tested sustainable corrosion inhibitor. The inhibitory action of corn peptone was further confirmed by electrochemical measurements. For instance, an increase in corn peptone concentration led to a decrease in corrosion current density and an increase in the diameter of the capacitive loop in Nyquist plots. AFM patterns revealed a significant decrease in surface deterioration due to the formation of a protective film which prevented the corrosive ions from reaching the working electrodes.

ACKNOWLEDGMENTS

This study was supported by the University of Tabriz under contract number: 3406.

DATA AVAILABILITY STATEMENT

Data that support the findings of this study are available from the corresponding author upon reasonable request.

ORCID

Taher Rabizadeh http://orcid.org/0000-0003-3483-2764

REFERENCES

[1] S. Vikneshvaran, S. Velmathi, *Mater. Corros.* **2018**, *69*, 1084.
[2] P. M. Krishnegowda, V. T. Venkatesha, P. K. M. Krishnegowda, S. B. Shivayogiraju, *Ind. Eng. Chem. Res.* **2013**, *52*, 722.
[3] J. Vogelsang, W. Strunz, *Mater. Corros.* **2001**, *52*, 462.
[4] K. Bundschuh, M. Schütze, *Mater. Corros.* **2001**, *52*, 204.
[5] Y. Bu, J. P. Ao, *Green Energy Environ.* **2017**, *2*, 331.
[6] L. Zhao, H. K. Teng, Y. S. Yang, X. Tan, *Mater. Corros.* **2004**, *55*, 684.
[7] A. Aouniti, N. Arrousse, F. El-Hajjaji, R. Salghi, M. Taleb, S. Kertit, L. Bazzi, B. Hammouti, *Arab. J. Chem. Environ. Res* **2017**, *4*, 18.
[8] P. B. Raja, M. Ismail, S. Ghoreishiamiri, J. Mirza, M. C. Ismail, S. Kakooei, A. A. Rahim, *Chem. Eng. Commun.* **2016**, *203*, 1145.
[9] I. W. Ma, S. Ammar, S. S. Kumar, K. Ramesh, S. Ramesh, *J. Coat. Technol. Res.* **2022**, *19*, 241. https://doi.org/10.1007/s11998-021-00547-0

[10] G. Weijie Guo, X. Zhao, D. Wang, Y. Li, L. Zhou, Z. Li, Y. Gao, *Russ. J. Electrochem.* **2021**, *57*, 970.
[11] B. J. Usman, S. A. Umoren, Z. M. Gasem, *J. Mol. Liq.* **2017**, *237*, 146.
[12] H. Ouici, M. Tourabi, O. Benali, C. Selles, C. Jama, A. Zarrouk, F. Bentiss, *J. Electroanal. Chem.* **2017**, *803*, 125.
[13] J. Lazrak, E. Ech-chihbi, R. Salim, T. Saffaj, Z. Rais, M. Taleb, *Colloids Surf. A* **2023**, *664*, 131148.
[14] L. I. N. Ezemonye, D. F. Ogeleka, F. E. Okieimen, *Chem. Ecol.* **2007**, *23*, 131.
[15] T. Rabizadeh, A. Matin Javid, M. Kazemi, N. Vahedian Khezerlou, H. Ghanbari, *Mater. Corros.* **2023**, *75*, 1521.
[16] H. Wei, B. Heidarshenas, L. Zhou, G. Hussain, Q. Li, K. Ostrikov, *Mater. Today Sustain.* **2020**, *10*, 100044.
[17] F. Figueredo, R. Vera, A. Molinari, *Mater. Corros.* **2020**, *71*, 663.
[18] L. Guo, S. T. Zhang, W. P. Li, G. Hu, X. Li, *Mater. Corros.* **2014**, *65*, 935.
[19] T. Rabizadeh, S. K. Asl, *J. Mol. Liq.* **2019**, *276*, 694.
[20] T. Rabizadeh, S. Khameneh Asl, *Mater. Corros.* **2019**, *70*, 738.
[21] F. Davami, F. Eghbalpour, L. Nematollahi, F. Barkhordari, F. Mahboudi, *Iran. Biomed. J.* **2015**, *19*, 194.
[22] D. Mahto, P. Rani, S. Mishra, G. Sen, *Ind. Crops Prod.* **2014**, *58*, 251.
[23] S. Yahya, N. K. Othman, A. R. Daud, A. Jalar, R. Ismail, *Anti Corros. Methods Mater.* **2015**, *62*, 301.
[24] P. Bothi Raja, M. G. Sethuraman, *Mater. Corros.* **2009**, *60*, 22.
[25] Z. Golshani, S. M. A. Hosseini, M. Shahidizandi, M. J. Bahrami, *Mater. Corros.* **2019**, *70*, 1862.
[26] I. Obot, N. Ankah, A. Sorour, Z. Gasem, K. Haruna, *Sustain. Mater. Technol.* **2017**, *14*, 1.
[27] G. Khan, W. J. Basirun, S. N. Kazi, P. Ahmed, L. Magaji, S. M. Ahmed, G. M. Khan, M. A. Rehman, A. B. B. M. Badry, *J. Colloid Interface Sci.* **2017**, *502*, 134.
[28] A. Yousefi, S. Javadian, J. Neshati, *Ind. Eng. Chem. Res.* **2014**, *53*, 5475.
[29] G. Gómez-Sánchez, O. Olivares-Xometl, P. Arellanes-Lozada, N. V. Likhanova, I. V. Lijanova, J. Arriola-Morales, V. Díaz-Jiménez, J. López-Rodríguez, *Int. J. Mol. Sci.* **2023**, *24*, 6291.
[30] O. Sanni, A. Popoola, O. Fayomi, *J. Bio- Tribo-Corros.* **2019**, *5*, 1.
[31] H. Zarrok, A. Zarrouk, R. Salghi, B. Hammouti, M. Elbakri, M. Ebn Touhami, F. Bentiss, H. Oudda, *Res. Chem. Intermed.* **2014**, *40*, 801.
[32] A. A. F. Sabirneeza, S. Subhashini, R. Rajalakshmi, *Mater. Corros.* **2013**, *64*, 74.
[33] I. B. Obot, N. O. Obi-Egbedi, *Colloids Surf. A* **2008**, *330*, 207.
[34] C. M. Fernandes, M. V. P. de Mello, N. E. dos Santos, A. M. T. de Souza, M. Lanznaster, E. A. Ponzio, *Mater. Corros.* **2020**, *71*, 280.
[35] F. El-Hajjaji, M. Messali, A. Aljuhani, M. R. Aouad, B. Hammouti, M. E. Belghiti, D. S. Chauhan, M. A. Quraishi, *J. Mol. Liq.* **2018**, *249*, 997.
[36] C. Kamal, M. G. Sethuraman, *Mater. Corros.* **2014**, *65*, 846.
[37] M. R. Ortega Vega, S. Mattedi, R. M. Schroeder, C. de Fraga Malfatti, *Mater. Corros.* **2021**, *72*, 543.
[38] N. Caliskan, E. Akbas, *Mater. Corros.* **2012**, *63*, 231.
[39] M. Pakiet, I. H. Kowalczyk, R. Leiva Garcia, R. Akid, B. E. Brycki, *J. Mol. Liq.* **2018**, *268*, 824.
[40] Q. Qu, Z. Hao, S. Jiang, L. Li, W. Bai, *Mater. Corros.* **2008**, *59*, 883.
[41] L. A. L. Guedes, K. G. Bacca, N. F. Lopes, E. M. da Costa, *Mater. Corros.* **2019**, *70*, 1288.
[42] A. Singh, Y. Lin, K. R. Ansari, M. A. Quraishi, E. E. Ebenso, S. Chen, W. Liu, *Appl. Surf. Sci.* **2015**, *359*, 331.
[43] S. M. R. Shoja, M. Abdouss, A. A. Miran Beigi, *Mater. Corros.* **2022**, *73*, 623.
[44] M. Yeganeh, I. Khosravi-Bigdeli, M. Eskandari, S. R. Alavi Zaree, *J. Mater. Eng. Perform.* **2020**, *29*, 3983.
[45] Y. Ye, D. Yang, H. Chen, S. Guo, Q. Yang, L. Chen, H. Zhao, L. Wang, *J. Hazard. Mater.* **2020**, *381*, 121019.
[46] O. M. A. Khamaysa, I. Selatnia, H. Zeghache, H. Lgaz, A. Sid, I.-M. Chung, M. Benahmed, N. Gherraf, P. Mosset, *J. Mol. Liq.* **2020**, *315*, 113805.
[47] S. K. Gupta, R. K. Mehta, M. Yadav, O. Dagdag, V. Mehmeti, A. Berisha, E. E. Ebenso, *J. Mol. Liq.* **2023**, *382*, 121976.
[48] E. E. Oguzie, *Mater. Chem. Phys.* **2006**, *99*, 441.
[49] R. Yıldız, *Corros. Sci.* **2015**, *90*, 544.

How to cite this article: T. Rabizadeh, *Mater. Corros.* **2024**, *75*, 1142–1154.
https://doi.org/10.1002/maco.202414346